BRAINLAB
Brain Research using Advanced Imaging in Neurology
UNIVERSITY OF LIVERPOOL
NHS
The Walton Centre
NHS Foundation Trust

Fischl B. FreeSurfer. NeuroImage 2012;62:774–81. https://doi.org/10.1016/j.neuroimage.2012.01.021.
Iglesias JE, Billot B, Balbastre Y, Tabari A, Conklin J, Gilberto González R, et al. Joint super-resolution and synthesis of 1 mm isotropic MP-RAGE volumes from clinical MRI exams with scans of different orientation, resolution and contrast. NeuroImage 2021;237:118206. https://doi.org/10.1016/j.neuroimage.2021.118206.
Jenkinson M, Beckmann CF, Behrens TEJ, Woolrich MW, Smith SM. FSL. NeuroImage 2012;62:782–90. https://doi.org/10.1016/j.neuroimage.2011.09.015.
Rebsamen M, McKinley R, Radojewski P, Pistor M, Friedli C, Hoepner R, et al. Reliable brain morphometry from contrast-enhanced T1w-MRI in patients with multiple sclerosis. Hum Brain Mapp 2022;44:970–9. https://doi.org/10.1002/hbm.26117.
Rebsamen M, Rummel C, Reyes M, Wiest R, McKinley R. Direct cortical thickness estimation using deep learning-based anatomy segmentation and cortex parcellation. Human Brain Mapping 2020;41:4804–14. https://doi.org/10.1002/hbm.25159.
Whelan CD, Altmann A, Botía JA, Jahanshad N, Hibar DP, Absil J, et al. Structural brain abnormalities in the common epilepsies assessed in a worldwide ENIGMA study. Brain 2018;141:391–408. https://doi.org/10.1093/brain/awx341.
Yao AD, Cheng DL, Pan I, Kitamura F. Deep Learning in Neuroradiology: A Systematic Review of Current Algorithms and Approaches for the New Wave of Imaging Technology. Radiology: Artificial Intelligence 2020;2:e190026. https://doi.org/10.1148/ryai.2020190026.

Reconstruction of 2D MRI using SynthSR and DL+DiReCT for Subcortical Shape Analysis in Epilepsy

Corey Ratcliffe[1,2], Christophe de Bezénac[1], Kumar Das[3], Anthony Marson[1], & Simon S. Keller[1]

1. Department of Pharmacology and Therapeutics, Institute of Systems, Molecular & Integrative Biology, University of Liverpool, U.K.
2. National Institute of Mental Health & Neuro Sciences (NIMHANS) Bangalore, India
3. The Walton Centre NHS Foundation Trust, Liverpool, U.K.

Deep learning-based image synthesis and segmentation methods have shown promise as a potential workaround for the loss of resolution in clinically-acquired 2D MRI scans. Structural comparisons suggest that volume and thickness estimates may not benefit from synthesised and resampled image approaches, and whilst reconstructed images may be more sensitive to morphometric differences than 2D scans, they may also be more susceptible to false positives. Reconstructed images should be used with caution.

Introduction

MRI acquired during routine clinical practice are often unsuitable for quantitative analyses, which have myriad advantages over qualitative evaluation. Two recent software packages (SynthSR and DL+DiReCT) have leveraged A.I. models in an attempt to ammeliorate the limitations of clinical MRI acquisition in quantitative structural analyses. Further studies are needed to validate the efficacy of these approaches in estimating isotropic (3D) cortical structures from anisotropic (2D) scans.

Methods

In the same scanning session, 2D- and 3D-T1w 3T MRI scans were acquired from 31 patients and 39 controls. DL+DiReCT (using nibabel) and SynthSR were used to synthesise 3D images from the 2D scans, which were preprocessed using the FSL-ANAT and FreeSurfer pipelines alongside the 3D scans. Dice coefficients and intraclass correlation coefficients were used to compare regionwise correspondence (spatial and volumetric) between the datasets. Subcortical shape differences were then estimated.

Results

When averaged across 166 cortical and subcortical parcellations derived from the Destrieux atlas and FreeSurfer aseg algorithm, the Dice coefficients between the 3D scans and the anisotropic/synthesised/resampled images were low (2D = 0.167, DL+DiReCT = 0.146, SynthSR = 0.156). Dice coefficients averaged from the remaining 15 subcortical structures were marginally higher (2D = 0.280, DL+DiReCT = 0.247, SynthSR = 0.262). Averaged regionwise comparisons of volumetry were high (volume over 181 regions and structures: 2D = 0.994, DL+DiReCT = 0.992, SynthSR = 0.988; thickness over 148 regions: 2D = 0.913, DL+DiReCT = 0.928, SynthSR = 0.807).

Intraclass correlation coefficients were used to measure the regionwise resemblance between metrics from the 3D scans and metrics from the anisotropic/synthesised/resampled images. Average ICCs were computed for the volumes of the 166 cortical regions (ICC: 2D = 0.677, DL+DiReCT = 0.620, SynthSR = 0.563), the volumes of the 15 subcortical regions (ICC: 2D = 0.685, DL+DiReCT = 0.684, SynthSR = 0.576), and the thicknesses of the 148 cortical regions (ICC: 2D = 0.399, DL+DiReCT = 0.344, SynthSR = 0.200).

Significant inwards surface deflation of the subcortical structures was detected in the 3D scans when the individuals with IGE (n = 31, males = 14, mean age = 32.16) were compared to controls (n = 39, males = 16, mean age = 32.13). In the 2D scans, no significant inwards deflation was detected, whereas the synthesised/upsampled images were more sensitive to the true positive results, as well as false negatives.

Conclusions

Regional spatial and volumetric measurements taken from synthesised images showed no improvement in correspondence with 'ground truth' 3D scans when compared to 2D scans. Subcortical surface shape analyses performed on synthesised images offered more sensitivity to true positive results than the 2D scans, at the cost of susceptibility to false positive and false negative results. Conclusions drawn from synthesised data should be interpreted with caution, but may provide a partial solution to issues of resolution-related lack of statistical power in clinical imaging analyses.

Figure 1. Schematic of the preprocessing pipeline used for the regional comparisons. Resampled/synthesised 3D images were generated from 2D scans using DL+DiReCT (nibabel) and SynthSR, and were processed using FreeSurfer's recon-all command. A comparable pipeline with FSL-ANAT and FSL-FIRST replacing FreeSurfer's recon-all was used for shape analysis.

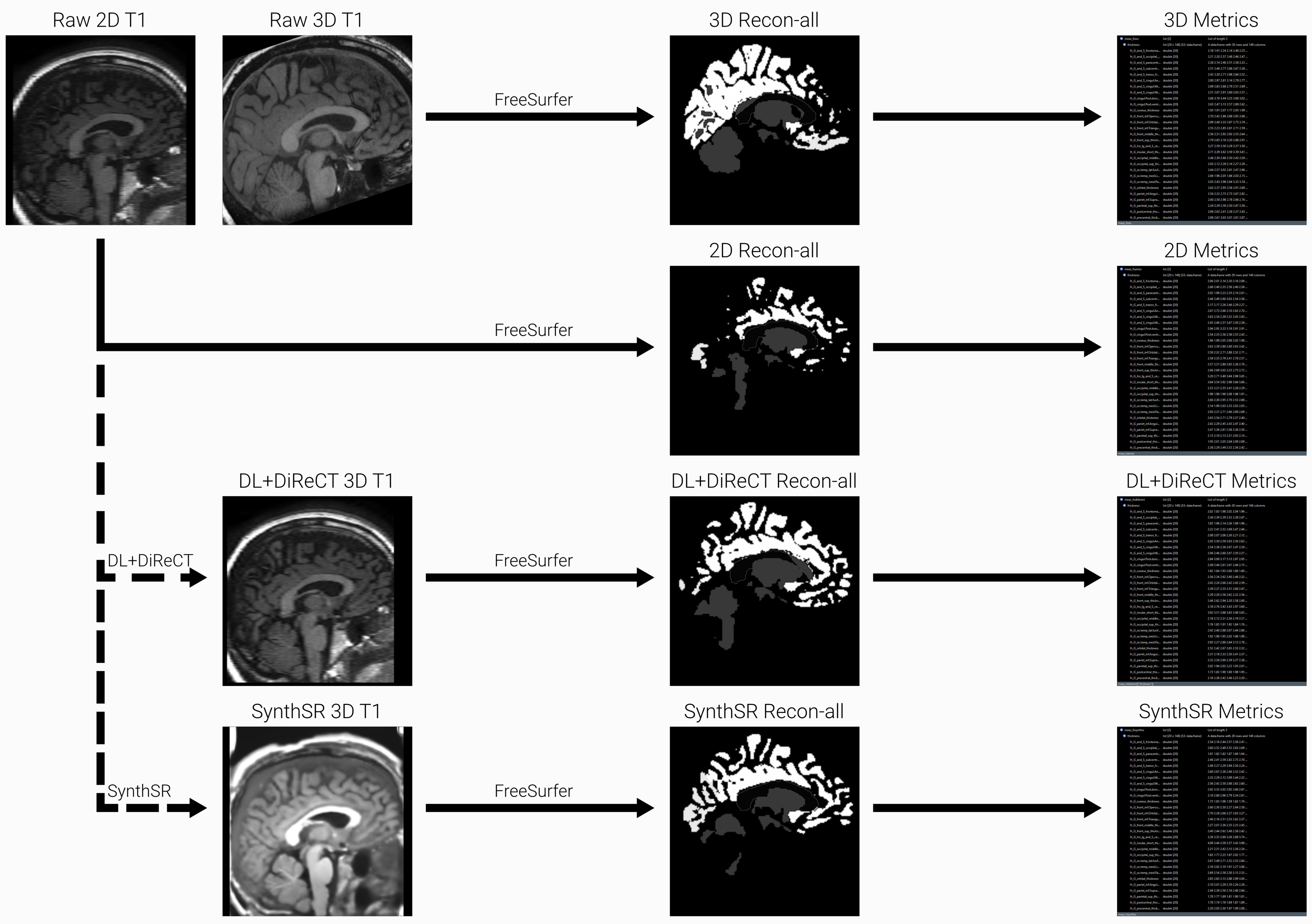

Figure 2 (R). Heatmaps representing segmentation dice coefficients across the 148 cortical regions and 33 subcortical regions from the Destrieux atlas and FreeSurfer aseg algorithm respectively. Averaged regionwise volume (cortical and subcortical) and thickness (cortical) correlation coefficients between the 3D scans and the 2D scans, DL+DiReCT images, and the SynthSR images in turn are also presented.

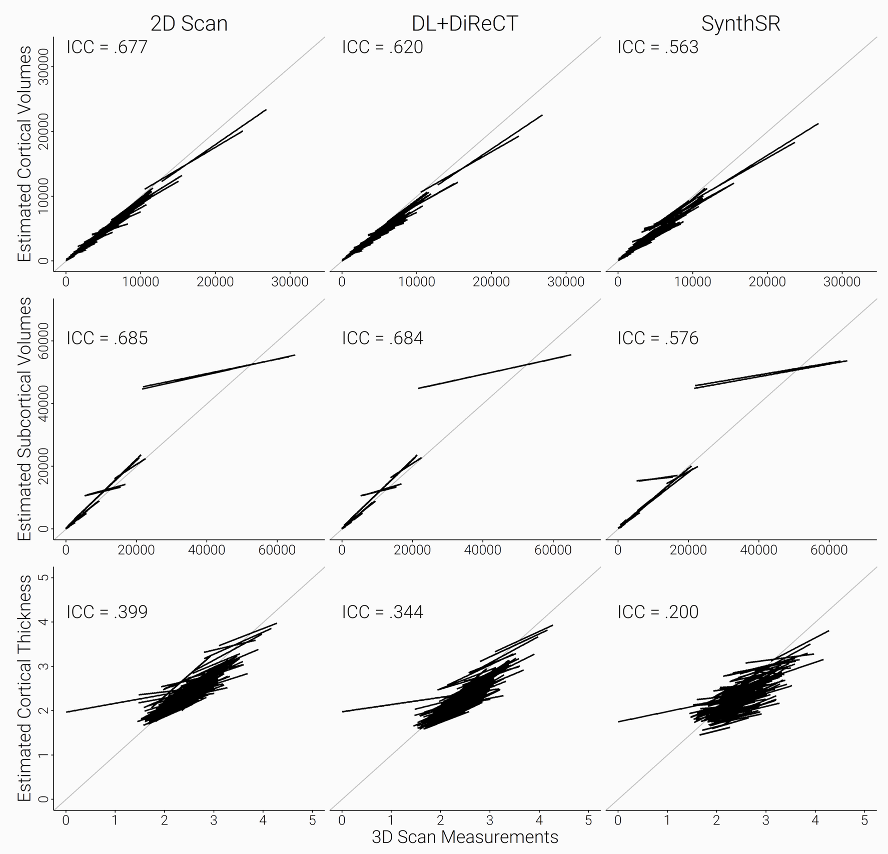

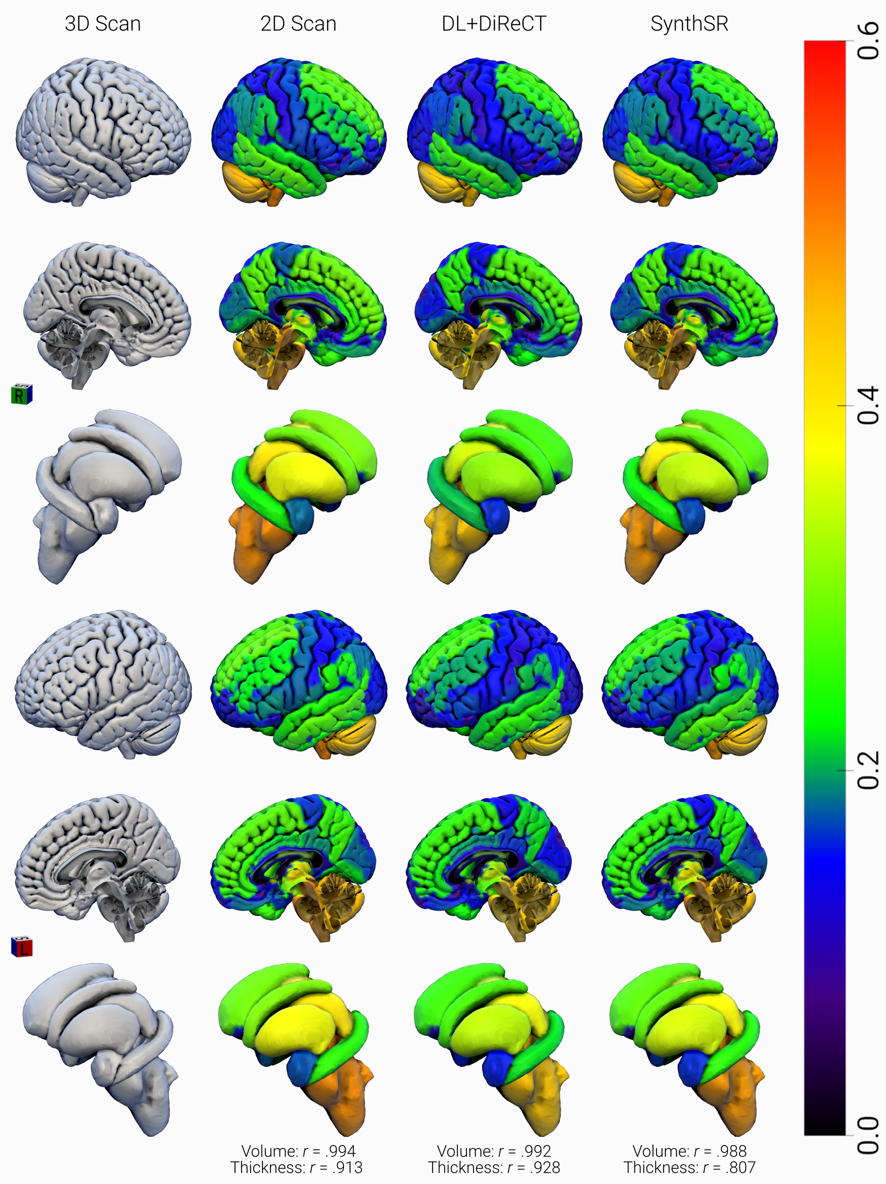

Figure 3 (L). Trend lines representing correlations between the regional volume and grey matter thickness measurements taken from the 3D scans, and the same volumes taken from the 2D scans, DL+DiReCT resampled images, and the SynthSR images in turn. Subcortical structure volume estimates are presented separately, average intraclass correlation coefficients are provided, and a line indicating proportionality (i.e. y = x) has been plotted for clarity.

	Accumbens (L)	Accumbens (R)	Amygdala (L)	Amygdala (R)	Caudate (L)	Caudate (R)	Hippocampus (L)	Hippocampus (R)	Pallidum (L)	Pallidum (R)	Putamen (L)	Putamen (R)	Thalamus (L)	Thalamus (R)
Raw 3D	0.974				0.900	0.959		0.815			0.966	0.954		0.986
Raw 2D								0.828						
DL+DiReCT					0.968					0.943	0.996			
SynthSR					0.966	0.918	0.931	0.981				0.977	0.982	

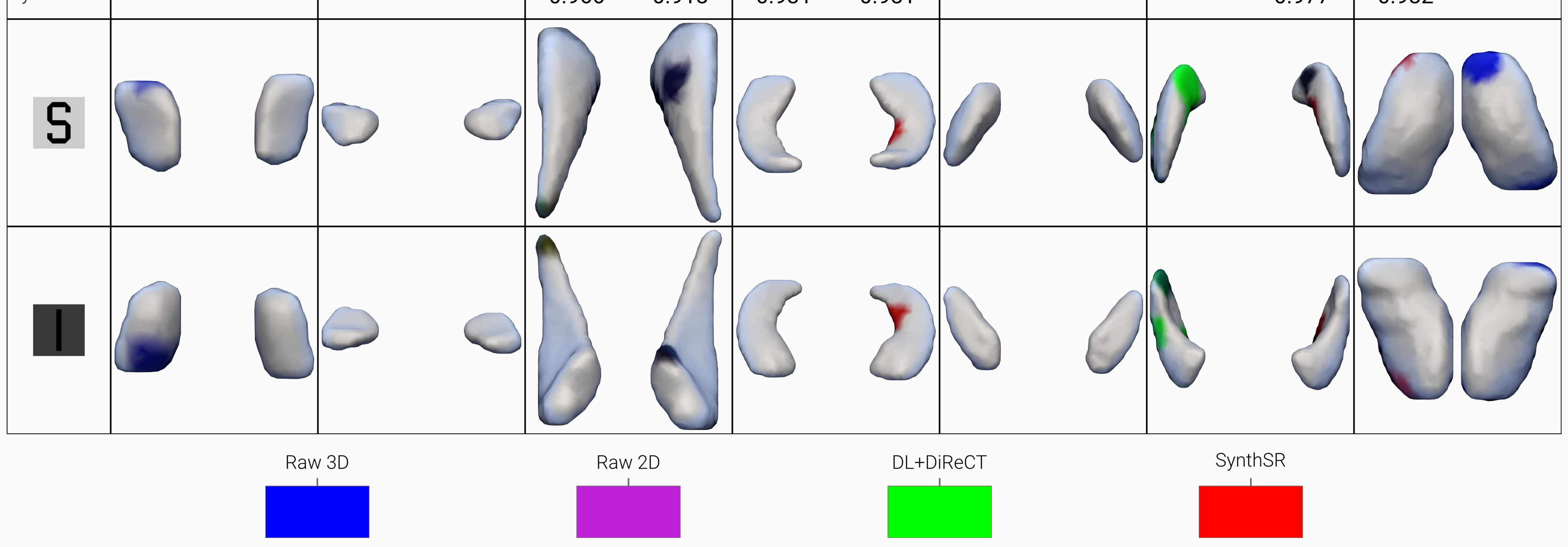

Figure 4. The maximum intensities of the regional surface deflations following 5000 permutations of FSL-randomise are shown in the table above. Intensity values are equal to 1 - p. Locations of the p-adj < .05 cluster-corrected thresholded shape changes (i.e. where the IGE group had significant inwards surface deflation compared to the controls) are shown, colour coded to the images from which they were derived.